

Supplement material

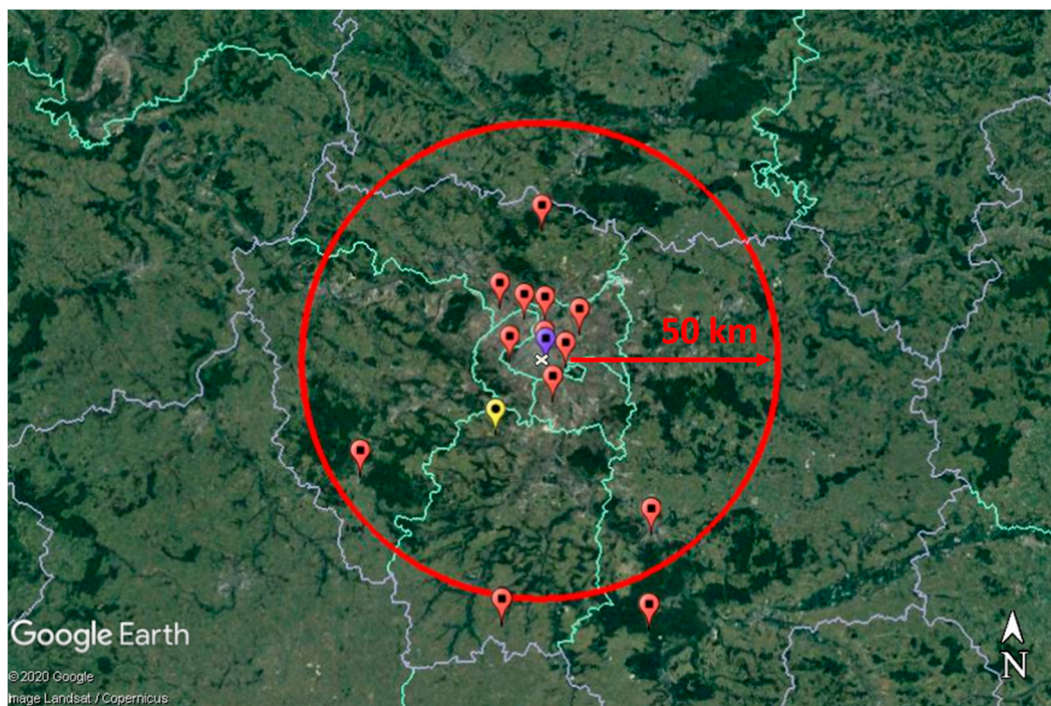


Figure S1. The domain of study around Paris (white cross) showing locations of the PM_{2.5} and NO₂ observations from the Airparif stations (red pins), PM composition observations at SIRTA (yellow pin), as well as NH₃ observations derived from the mini-DOAS instrument (blue pin) and from the IASI satellite instrument (inside the red circle). Map provided by Google Earth V7.3.2.5776, US Dept. of State Geographer, ©Google, 2020, Image Landsat/Copernicus, Data SIO, NOAA, US, Navy, NGA, and GEBCO.

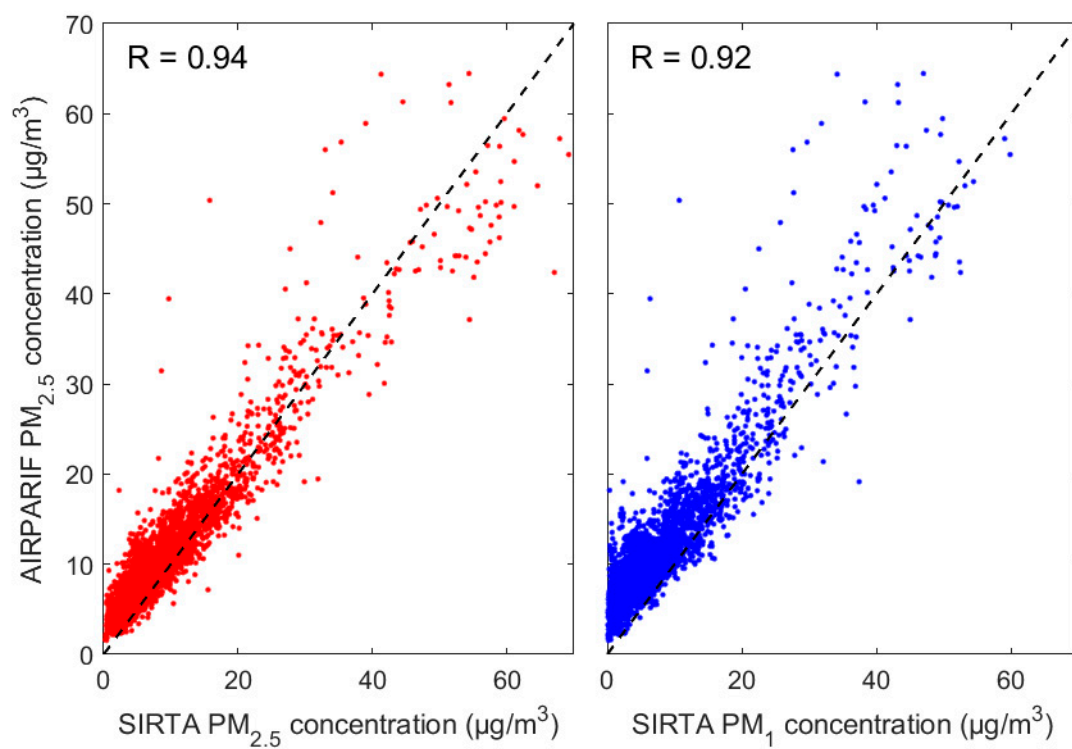


Figure S2. Correlation plots between hourly PM_{2.5} concentrations derived from the mean of the 13 Airparif stations and PM_{2.5} (red, left panel) and PM₁ (blue, right panel) concentrations measured at SIRTA. PM_{2.5} and PM₁ concentrations measured at SIRTA are strongly correlated with the average of measurements at all the Airparif stations with $R = 0.94$ and $R = 0.92$ (p -value < 0.05).

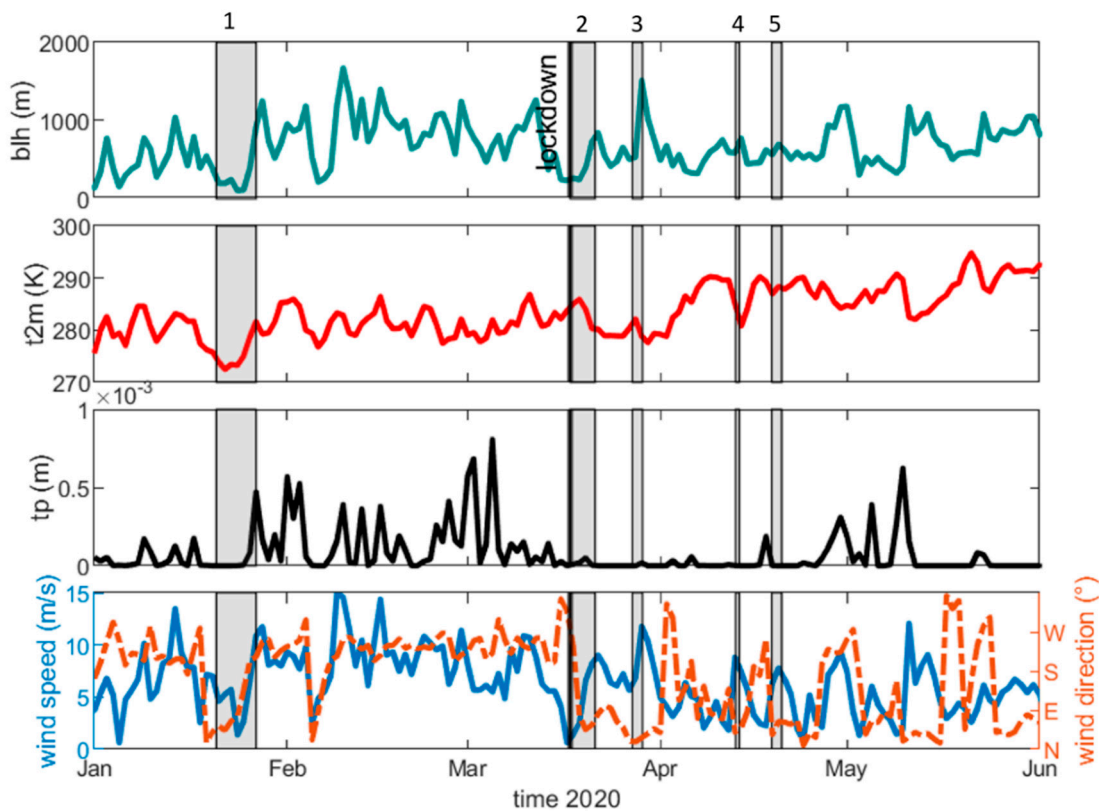


Figure S3. Timeseries of daily meteorological parameters over Paris from January to June 2020 and for the 5 investigated periods in shaded grey: boundary layer height (in meter; dark cyan, upper panel), temperature at 2 meters (in Kelvin; red, upper middle panel), total precipitation (in meter; black, lower middle panel), and wind speeds and directions (blue and orange in lower panel) derived from the ECMWF ERA-5 (C3S, 2021).

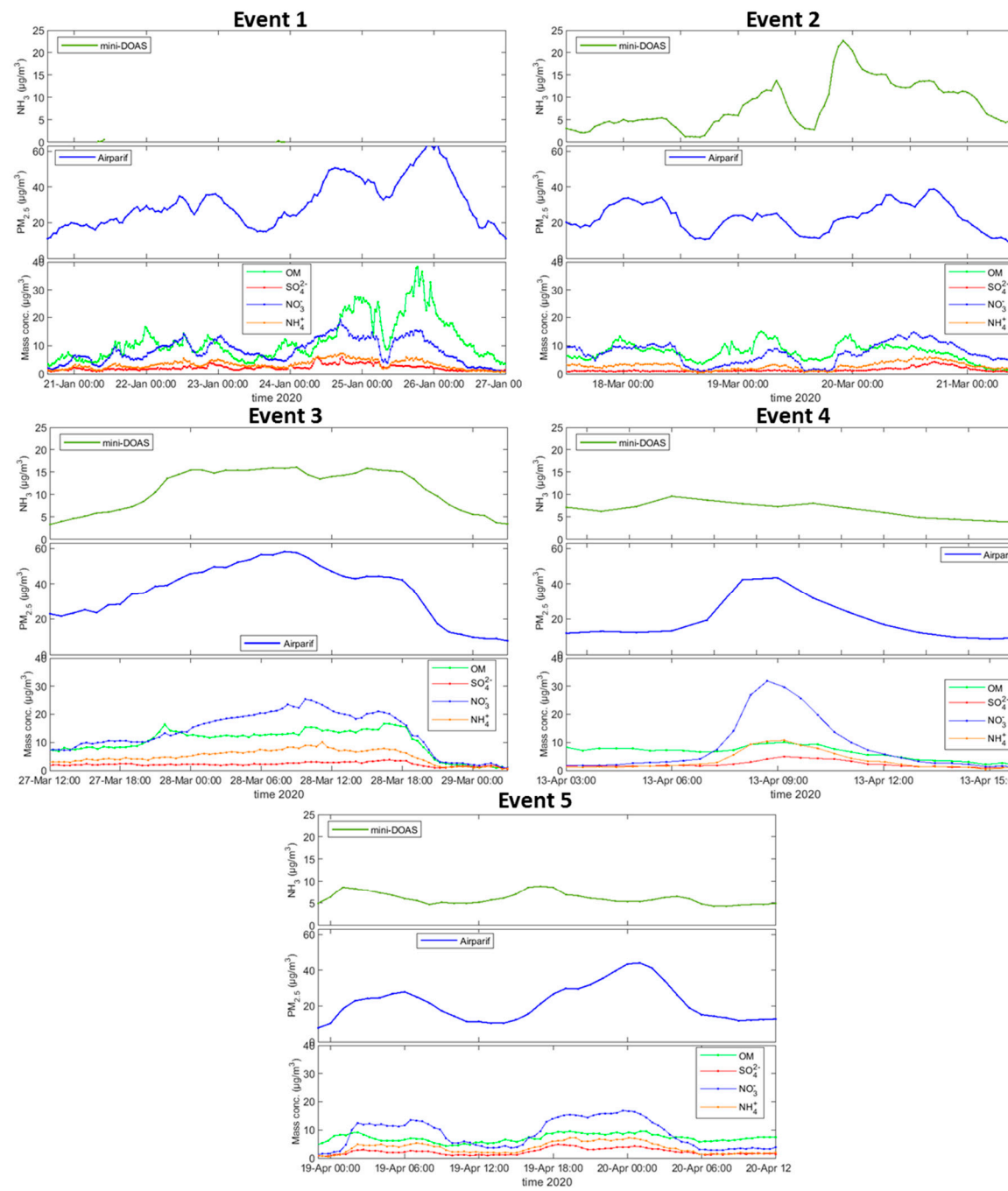


Figure S4. Timeseries of NH_3 , $\text{PM}_{2.5}$ and major submicron chemical species concentrations over Paris during the five periods investigated.

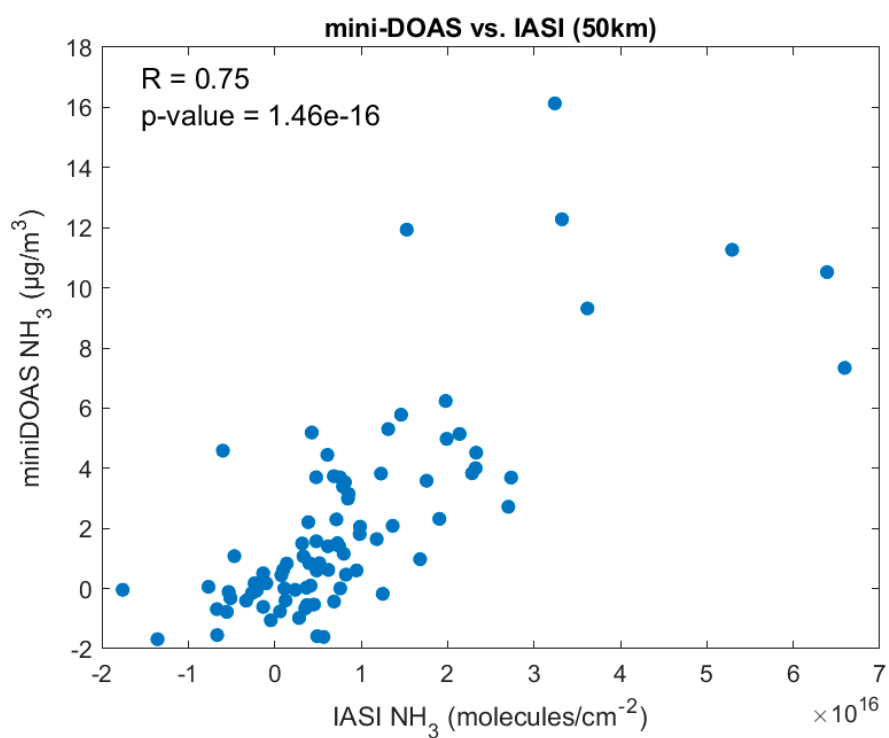


Figure S5. IASI and mini-DOAS NH₃ comparison.

Pearson's correlation $R = 0.75$ ($p\text{-value} < 1.10 \cdot 10^{-16}$) over 85 days of comparisons using coincidence criteria:

- Spatial: IASI pixels are average within a 50-km radius circle around Paris.
- Temporal: mini-DOAS data are taken within the same hour as the IASI satellite overpass time (mean of IASI A, B, and C).

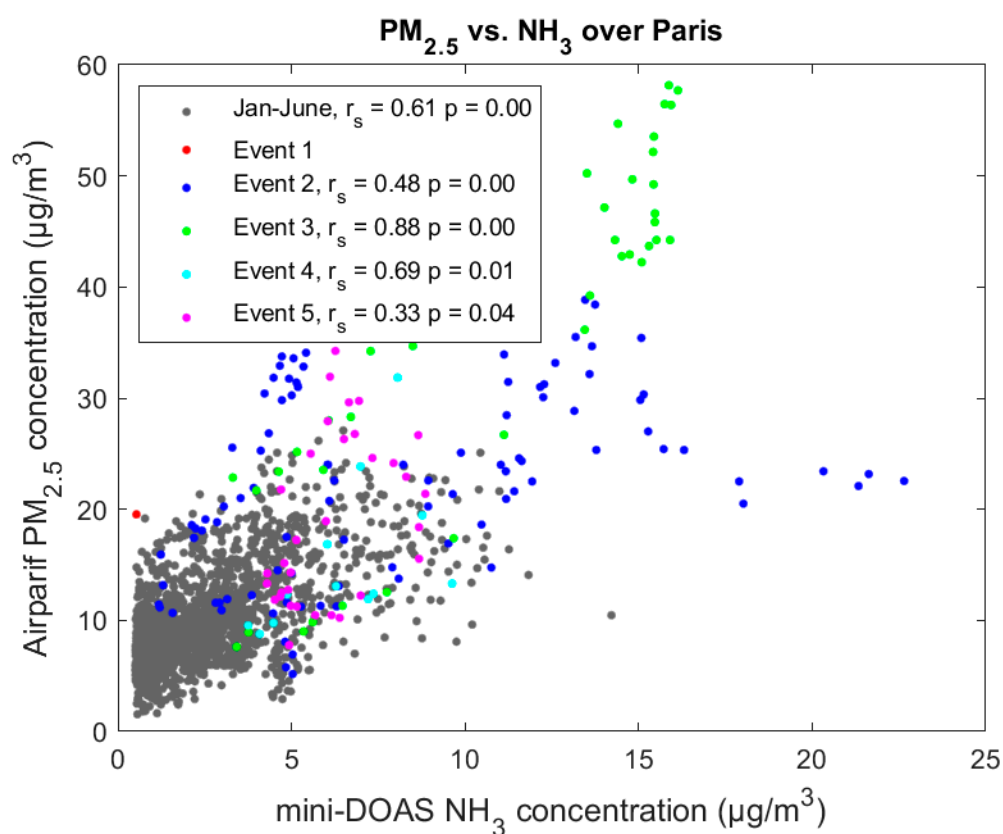


Figure 6. Correlation plot (using Spearman's rank correlation coefficient) between hourly PM_{2.5} and NH₃ concentrations over Paris during the period of study (January-June 2020 in grey), color-coded according to the five periods investigated. NH₃ concentrations derived from the mini-DOAS below detection limits have been discarded.

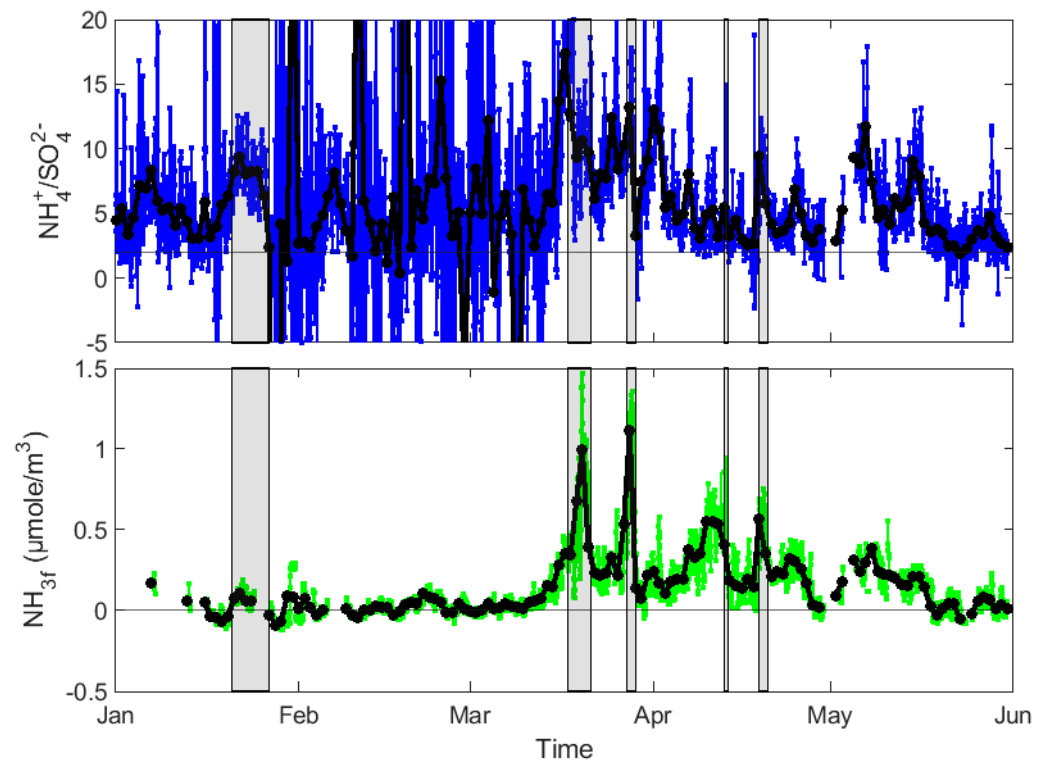


Figure 7. Hourly (blue) and daily (black) NH_4^+ to SO_4^{2-} molar concentrations ratio (upper panel), and hourly (green) and daily (black) free total ammonia concentrations ($\mu\text{mole}/\text{m}^3$) defined as $\text{NH}_{3f} = \text{NH}_3 + \text{NH}_4^+ - 2 \times \text{SO}_4^{2-}$ (lower panel) as function of time.

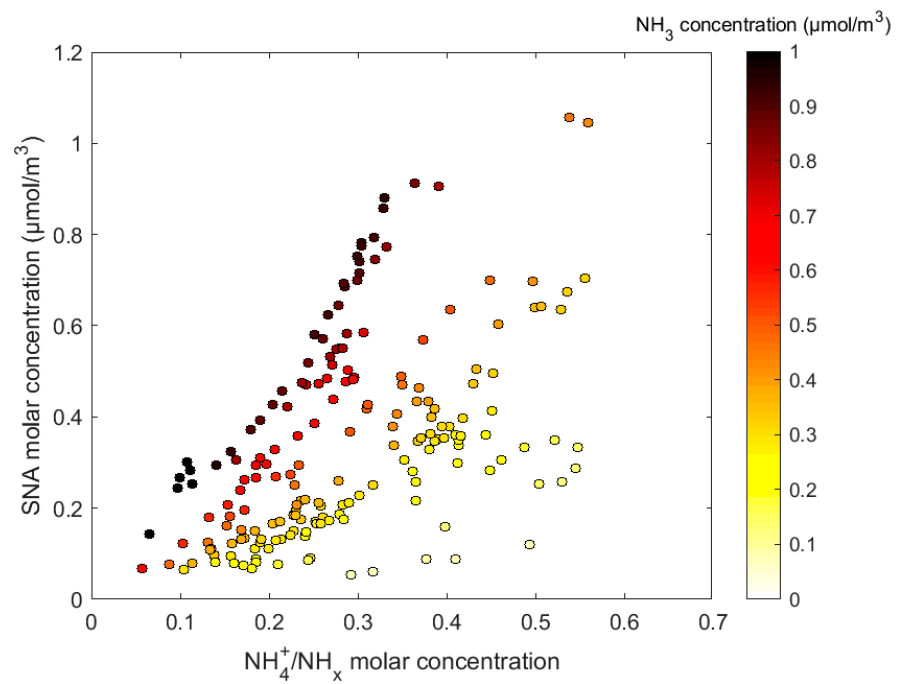


Figure S8. Relationship between the conversion rate of ammonia to ammonium ($\text{NH}_4^+/\text{NH}_x$) and Scheme 3. during pollution episodes occurring in spring 2020.

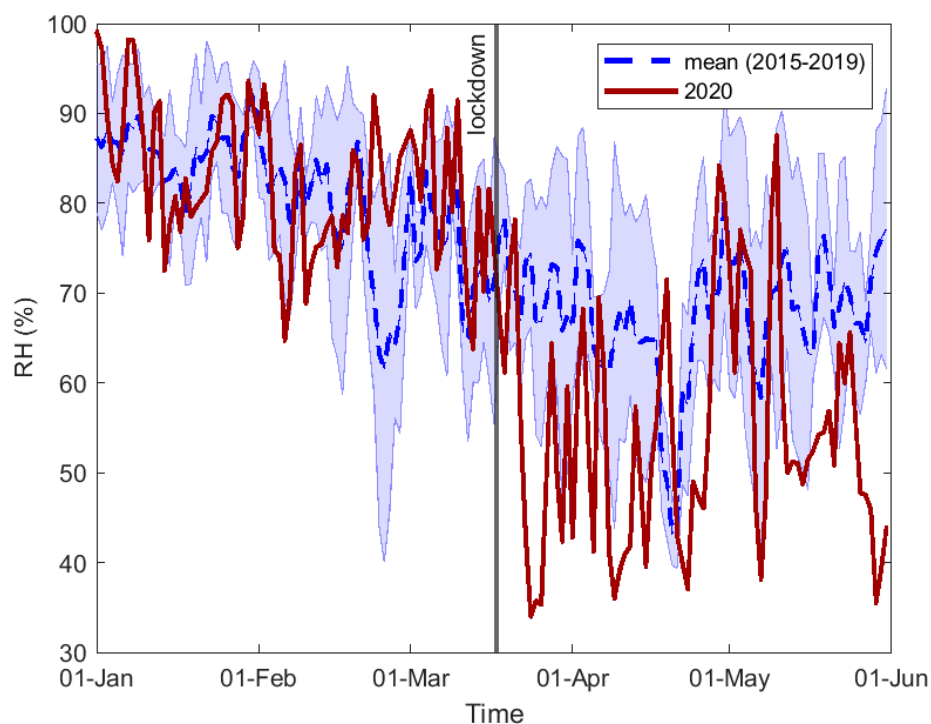


Figure 9. Daily concentrations of RH (%) measured in Paris from January to June of 2020 (solid lines), and average from 2015 to 2019 (dashed lines). Light blue area represents the 1- σ standard deviation around the 5-year average. The vertical line corresponds to the start of the lockdown period in France.